ELSEVIER

Polymer 40 (1999) 2347–2365

polymer

Toughness mechanism in semi-crystalline polymer blends: II. High-density polyethylene toughened with calcium carbonate filler particles

Z. Bartczak[1a], A.S. Argon[a,*], R.E. Cohen[a], M. Weinberg[b]

[a]*Massachusetts Institute of Technology, Cambridge, MA 02139, USA*
[b]*E.I. du Pont de Nemours & Co., Central Research and Development, Experiment Station, Wilmington, DE 19898, USA*

Received 12 December 1997; revised 1 May 1998; accepted 2 June 1998

Abstract

Here we extend the investigation described in the preceding companion communication. To rectify its notch brittleness, high-density polyethylene (HDPE) was modified by rigid particulate fillers consisting of three different sizes of $CaCO_3$ particles of 3.50, 0.70 and 0.44 μm weight average diameter in various volume fractions. Mechanical properties including notched Izod impact energy of the extrusion-blended/injection-moulded samples were examined as a function of filler particle size and filler volume fraction. In exactly the same manner as exhibited by the rubber particle-modified compositions described in the previous communication, the toughness of the $CaCO_3$-filled materials increased dramatically when the mean interparticle ligament thickness of the matrix polyethylene dropped to values below 0.6 μm. The stiff fillers used in this study provided the unusual additional benefit of substantially increasing the Young's modulus of the compounds while also dramatically improving their impact energy.

Keywords: Toughness; Semi-crystalline polymer; Filler particles

1. Introduction

One common purpose for adding mineral fillers to polymers is cost reduction. Fillers have also been used increasingly to fulfil additional roles, such as enhancing stiffness, decreasing dielectric loss or increasing absorption of infrared radiation [1]. However, the prevailing opinion is that addition of rigid, inorganic fillers to polymers will generally have embrittling effects by sharply decreasing their impact energy, and should be avoided

In fact, most of the studies of modification of semi-crystalline polymers with rigid particulate fillers report a significant decrease of toughness compared to neat polymers. There are, however, several studies demonstrating an increase in toughness with rigid particle fillers in certain systems such as, e.g., filled polypropylene [2,3] and filled polyethylene [3–9]. An impressive increase of impact energy by a factor of nearly 4 was reported by Wang and co-workers [6–10] for polyethylene filled with calcium carbonate particles.

In the preceding companion communication [11], called hereafter (I), we discussed the toughening mechanism of HDPE with a variety of rubber particles and drew attention to its possible more far-reaching application to other semi-crystalline polymers. On the basis of a pioneering investigation of rubber-modified Nylon 6,6, Wu [12] proposed a criterion of toughening of such polymers by rubber particles, in which for a blend to be tough the interparticle matrix ligament thickness in it has to be smaller than a certain critical value, characteristic for a given matrix polymer. Based on the findings of Wu and detailed mechanical and microstructural/morphological studies of similar Nylon 6,6-EPDM rubber blends Muratoglu et al. [13] proposed a novel mechanism of toughening of semi-crystalline polymers by rubber particles. In (I) we demonstrated that the mechanism of Muratoglu et al. is also fully effective in toughening of HDPE by rubber particles of arbitrary properties, provided the criterion of Wu is satisfied.

The model proposed by Muratoglu et al. [13] was derived from the meticulously documented observation that crystallization of semi-crystalline polymers near the incoherent interface of particles leads to the formation of a layer of preferentially oriented crystallites which was found to be approximately 0.15 μm thick for Nylon 6 [14]. The lamellar

* Corresponding author.
[1] Permanent address: Centre of Molecular and Macromolecular Studies, Polish Academy of Sciences, 90-363 Lodz, Poland.

0032-3861/99/$ - see front matter
PII: S0032-3861(98)00444-3

crystallites are oriented within that layer with their low-energy, low plastic resistance (001) planes in the Nylon 6 lying parallel to the interface. In a separate companion study, related to the present communication to be referred to as (III) hereafter, we have made similar detailed morphological observations that nearly identical forms of preferential crystallization also occurs in HDPE from incoherent interfaces where, however, the thickness of the oriented near-interface crystalline layer has a thickness of 0.3–0.4 μm [15]. This phenomenon leads to the formation of a specific micro-orientation morphology in particle-modified semi-crystalline polymers, consisting of (i) particles (of rubber), (ii) oriented layers of the matrix crystallites around particles and (iii) randomly oriented bulk matrix outside the preferred crystallization layer. When the volume fraction of particles is low for a given particle size the oriented layers of the matrix surrounding the particles are separated from each other by unoriented bulk matrix, and a morphology of relatively high plastic resistance dominates the mechanical response of the material, resulting in premature fracture from unavoidable microstructural flaws and in brittle behaviour. On impact loading the resulting toughness of the modified polymer then is no better than that of the unmodified matrix. However, when the volume fraction of particles increases the oriented matrix shells around inclusions come into contact and the matrix ligaments between inclusions become filled completely with the well-oriented crystalline material of reduced plastic resistance which then percolates through the whole blend, and results in massive plastic flow by shear of the oriented ligaments. Thus, under impact loading a super-tough response of the blend, with up to 20-fold increase of impact energy results [13].

The Muratoglu et al. model of toughening of semi-crystalline polymers outlined above predicts the possibility of a super-tough behaviour of semi-crystalline polymers modified not only with rubber particles but also with stiff inorganic filler particles. According to this mechanism the primary role of the filler particles (rubber or otherwise) is to merely introduce into the semi-crystalline matrix appropriate volume concentrations of interface, distributed randomly in the matrix. The presence of these interfaces then alters the crystallization process of the matrix, resulting in the formation of layers of oriented crystalline material endowed with reduced plastic shear resistance around the particles. It is such pedigreed layers that exclusively are responsible for the toughness jump when such material percolates through the structure. Thus, in the tough response the role of the rubber particles is passive. Apart from providing the interpenetrating layers of crystalline matrix around themselves, the only additional requirement from the particles is to cavitate at the start of deformation and thereby offer no constraint to the deforming matrix ligaments. Therefore, rubber particles could be replaced with particles of other mechanical properties, such as stiff mineral fillers, provided the percolation conditions of oriented crystalline matter is met and the particles debond from the matrix [14]. Such an extension of the method of toughening to inorganic fillers would overcome the main drawback of compromise of elastic properties of the blend with rubber and, on the contrary, would result in substantial improvement of the stiffness of the blend. Thus, polymers modified with stiff filler particles should demonstrate both very high toughness and markedly improved stiffness at the same time, above not only the neat matrix behaviour but even that modified by rubber particles.

Thus, the goal of the present study was to investigate this hypothesis of toughening of semi-crystalline polymers with stiff particles. For this purpose HDPE modified with calcium carbonate ($CaCO_3$) (CC) was selected as a system to furnish a direct contrast to the study presented in (I). The crystallization and mechanical behaviour of HDPE is well known, making the results more definitive. Calcium carbonate is a common filler that can be obtained in a variety of sizes and surface treatment. Many types of specially precipitated calcium carbonate filler particles have relatively regular, nearly equiaxed shapes. Moreover, the practical importance of the HDPE/CC system, and the possibility of significant enhancement of its impact energy, compared to the neat resin, reported already by others [3–10], made a choice of this system very attractive. In a separate communication [15], we report a detailed investigation of the crystalline morphology and near-interface orientation phenomena in thin polyethylene layers crystallized in contact with both rubber and calcite single-crystal surfaces. The toughness of the blends of the present study will be discussed also in the light of the findings of the above mentioned study of crystallization habits around calcite surfaces.

2. Experimental procedure

2.1. Sample preparation

The polymer used in this study was high-density polyethylene (HDPE) Dowlex® IP-10, supplied by Dow Chemical Co. It has a density of 0.962 g/cm^3 (annealed) and a melt flow index of 9 g/10 min (2.16 kG at 190°C). Three types of calcium carbonate (CC) particles were used as fillers. The properties of these filler particles are listed in Table 1. The CC1 and CC2 particles were surface treated with calcium stearate by the manufacturer, while the CC3 particles had no surface treatment. The blends of HDPE with various CC particles ranging in volume fraction from 0 to 0.3 (i.e. containing from 0 to 0.55 weight fraction of CC particles) were prepared in two steps. First, polymer pellets were pre-mixed with CC powder in desired proportions and then mixed in the molten state, in a 28 mm Werner and Pfleider twin-screw extruder. The extrusion-mixing process was performed at temperatures within the range of 190–200°C and a rotation speed of the screws of 200 rpm. In an attempt to improve dispersion of CC3 particles (which had no

surface treatment) in the HDPE matrix, stearic acid in the amount of 4 wt.% (with respect to the weight of the filler particles) was added in the pre-mixing step.

The preparation of the test specimens from the compounded blends is described in detail in (I) [11].

2.2. Property measurements

The techniques used to characterize the blend samples included: differential scanning calorimetry (d.s.c.), tensile testing, notch Izod impact testing, scanning electron microscopy (SEM) and wide-angle X-ray scattering (WAXS). The description of the equipment used and procedures, except WAXS, are given in (I) [11].

The measurements of orientation, using WAXS were performed on a Rigaku horizontal goniometer, equipped with pole figure attachment, coupled to a Rigaku RU200 rotating anode X-ray generator with fine point source (Cu Kα radiation, filtered by a Ni filter and electronically). An accelerating voltage of 50 kV and tube current of 60 mA were used. The samples for X-ray diffraction measurements were machined out from the Izod bars in order to expose the core of these injection-moulded samples and to obtain sufficiently thin specimens for measurements in the transmission mode. The pole figures of the (110) and (200) planes of polyethylene, as well as the (104) plane of calcite, were determined. The diffraction intensity data were collected at a fixed Bragg angle, corresponding to the position of the diffraction peak of the plane of interest, while polar angle, α, and azimuthal angle, β, of the sample cradle were changed stepwise (in increments of 5°) in the range from 0 to 90° and from 0 to 360°, respectively. To construct full pole figures it was necessary to collect data in both transmission and reflection modes. The connection angle, α_c, at which the data from the transmission and reflection modes were connected, was 50°. The pole figures were calculated from the collected data after application of all necessary corrections for background scattering, sample absorption and instrumental defocusing. For plotting, the polar orientation distribution (POD) program, a part of the so-called popLA package (Los Alamos National Laboratory, Los Alamos, NM) was used.

3. Experimental results

3.1. Characterization of fillers and their dispersion in HDPE

Table 1 presents the properties of three types of calcium carbonate fillers selected for use in this study labelled as CC1, CC2 and CC3. Fig. 1 presents representative SEM micrographs of the CC fillers. In addition to the volume fraction of the filler, from the point of view of the performance of a composite, the mean size, the size distribution, as well as the shape of the particles, are of importance. If the mechanism of toughening is similar to that of rubber particles, as was assumed, it can be expected that for a given volume fraction the smaller the mean size of particles and the narrower the size distribution, the more effectively the particles will enhance the toughness of the matrix [12,13]. The shape of the particles probably also plays a role. It may be guessed that particles with more regular shapes should be more effective at a given size and volume fraction. Taking into consideration the size of the particles, the toughening efficiency of the fillers, at a given volume fraction, can be expected to be in the order of CC1 $<$ CC2 $<$ CC3. On the other hand CC3 particles had a significantly broader size distribution than CC2 particles, with a larger fraction of particles having relatively large sizes. In addition, the CC3 particles showed a strong tendency to agglomerate (see Fig. 1c), since no surface treatment had been applied to them. This was most likely the source of the poor performance of blends containing these particles.

Examination by SEM of fracture surfaces of the blends of HDPE containing these three families of filler demonstrated

Table 1
Characteristics of calcium carbonate fillers used in this study

Filler code	Trade name	Supplier	Type and source	Density (g/cm^3)	Mean size of particles (by weight)[a,b] (μm)	Surface area[a] (m^2)/g	Mean size of particles (by number)[b,c] (μm)	Geometrical standard deviation	Surface treatment
CC1	Hipflex 100	Specialty Minerals Inc., USA	Ground limestone, Adams (MA)	2.7	3.50	3	0.85	2.98	Calcium stearate
CC2	Superpflex 200	Specialty Minerals Inc., USA	Precipitated	2.7	0.70	7	0.41	1.61	Calcium stearate
CC3	Setacarb OG	Plüss-Staufer AG, Switzerland	Ground limestone, Orgon (France)	2.7	0.44		~0.15	2.47	Not treated

[a]Supplier data (weight-average particle size).
[b]Geometrical mean
[c]Estimated from size distibutions provided by supplier (number average particle size)

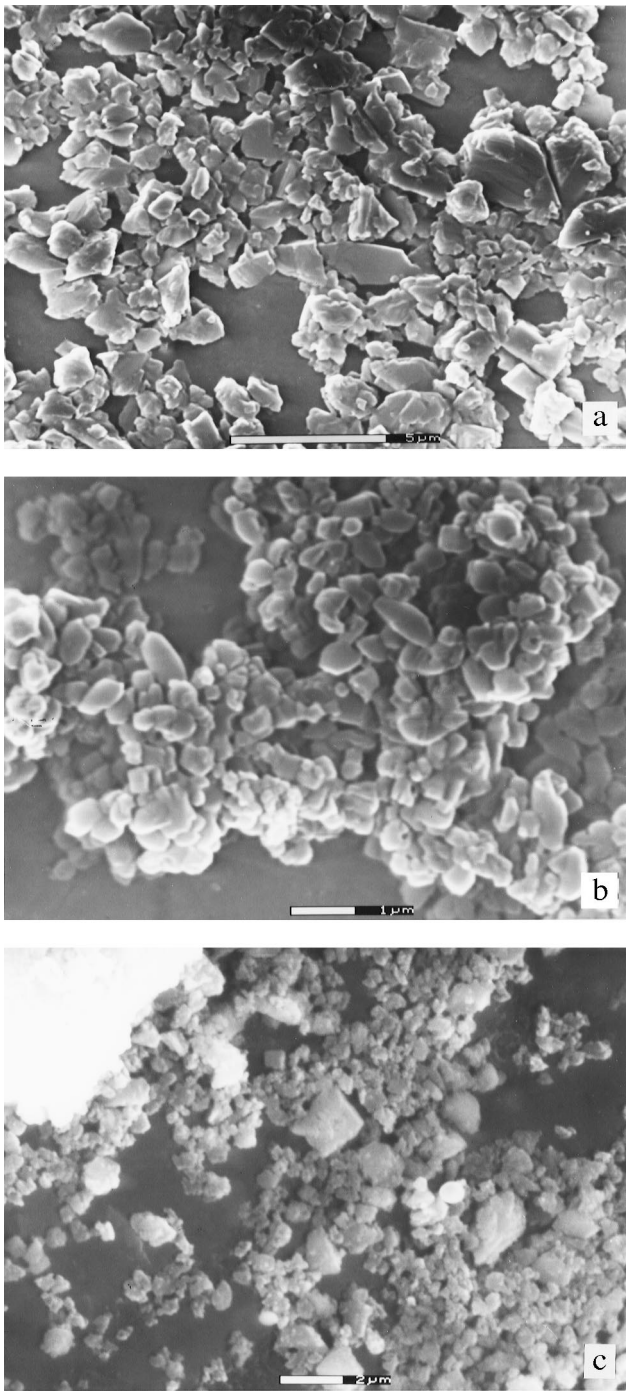

Fig. 1. SEM micrographs of the calcium carbonate fillers used for HDPE modification: (a) CC1, (b) CC2, (c) CC3. Note different magnification of micrographs; scale bar shown on each micrograph.

that the dispersion of CC1 and CC2 particles with calcium stearate-treated surfaces was very good up to filler concentrations of 25 vol% (i.e. 48 wt.%). Dispersion of CC2 filler worsened in the blend with particle concentration of 30 vol.%, where a tendency toward flocculation and aggregation of particles was observed. Dispersion of CC3 particles without surface modification was much poorer than CC1 or CC2 blends and contained numerous large dense agglomerates in the size range of 20 μm. These agglomerates were quite similar to those in the original CC3 powder before mixing, shown in Fig. 1c, which suggests that the shear forces in the extrusion and injection-moulding processes were too weak to break-up these agglomerates. The attempt to improve the dispersion of this filler by separately adding stearic acid to the mixture prior to extrusion proved to be completely ineffective.

3.2. Thermal analysis

In order to study the influence of CC filler on the crystallization of HDPE in the blends, d.s.c. studies of non-isothermal crystallization and melting behaviour were performed. Both cooling and heating scans were carried out with a rate of 10°C/min.

Table 2 presents the d.s.c. data for non-isothermal crystallization and melting, obtained for the blends with CC1, CC2 and CC3 fillers at various compositions. These data demonstrate that CC1 filler has some influence on nucleation of polyethylene crystallites by increasing the crystallization temperature by more than 1°C, while CC2 and CC3 induce only very slight increases of crystallization temperature in the range of 0.2–0.3°C, demonstrating very weak influence on the kinetics of crystallization of polyethylene. Some differences between neat HDPE and the blends can also be observed in melting behaviour. All blends have their melting curves shifted toward lower temperature, demonstrating that the lamellar crystallites in the blends melt at lower temperature, which indicates that they are thinner than the lamellae in neat HDPE. Such a thickness dependence of melting of PE crystallites is well documented [16].

In order to learn more about the size differences of crystallites, ‘difference curves’ were constructed from the melting curves of blends and neat HDPE, by subtracting from a melting curve of a particular blend that of neat HDPE (both normalized to unit mass of polyethylene in the samples). Such difference curves can provide information on difference of distribution of lamella sizes in the compared samples. Representative difference curves obtained for the blends containing 25 vol.% of CC are presented in Fig. 2. These curves imply that HDPE/CC blends contain crystallites of smaller thickness than neat HDPE but this is apparently compensated by larger number densities of thinner crystallites. The deviation of lamellar size distribution increases with increasing specific surface area of the filler, i.e. decreasing mean particle size. Additionally, the difference curves for all fillers show a long tail in the low temperature region, which suggests the presence of a fraction of very thin crystallites in the filled samples. The large difference between CC-filled and neat HDPE can also be seen in the degree of crystallinity of HDPE in these materials. The degree of crystallinity increases markedly, by up to 8%, with an increase of the content of CC in the blend and, particularly, with increasing specific surface area of the filler (decreasing mean particle size). In order to confirm

Table 2
D.s.c. crystallization and melting data (cooling and heating rate, $dT/dt = 10°C/min$)

Blend	Volumetric composition (PE/CC)	Crystallization		Melting		
		T_c (onset) (°C)	T_c (peak) (°C)	T_m (onset) (°C)	T_m (peak) (°C)	X^a (%)
HDPE (control)	100:0	122.3	119.7	125.8	132.4	72.1
HDPE/CC1	90:10	122.8	120.4	125.5	132.1	74.5
	80:20	123.2	120.7	125.5	132.4	79.1
	75:25	123.3	121.3	125.5	131.9	79.4
	70:30	123.5	121.4	125.5	131.9	80.4
HDPE/CC2	95:5	122.3	119.3	125.3	132.5	73.8
	90:10	122.3	119.9	125.3	131.6	75.3
	85:15	122.1	119.6	125.5	131.8	75.3
	80:20	122.4	120.0	125.2	131.5	79.4
	75:25	122.5	119.9	125.5	131.9	79.6
	70:30	122.3	119.9	124.8	131.7	79.8
HDPE/CC3	75:25	122.5	120.1	125.5	131.5	80.0

[a]Crystallinity of HDPE

such large increases of crystallinity in filled samples, additional measurements of crystallinity using X-ray diffraction were carried out. These measurements (not shown here) confirmed the d.s.c. results and, moreover, demonstrated that in the HDPE/CC blends the fraction of monoclinic modification of PE increases substantially. While in neat HDPE monoclinic modification constitutes 1–2% of the crystalline phase, in blends of high CC content it reaches levels of 3–6% of the crystalline phase.

We conclude from the d.s.c. studies that the presence of CC filler markedly influences the crystallization behaviour of HDPE. This influence manifests itself mostly in increasing degrees of crystallinity with a simultaneous reduction of the thickness of lamellae and formation of a new fraction of very thin crystallites. Since the crystallization of polyethylene in the blend samples proceeds at slightly higher temperatures than in neat HDPE, apparently due to a weak influence of CC particles on nucleation, an opposite effect,

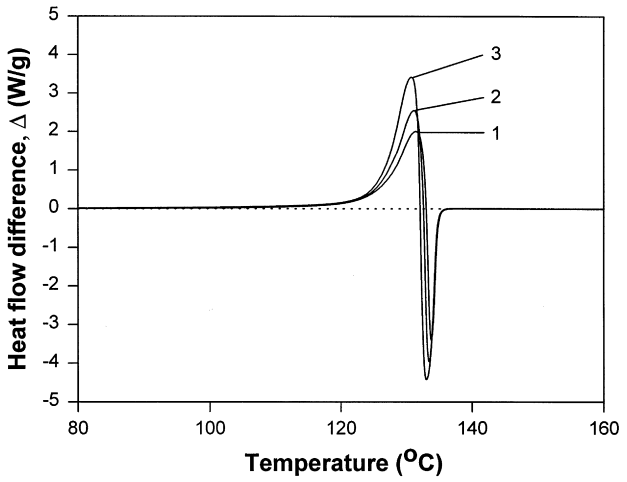

Fig. 2. D.s.c. difference curves of melting of the blends containing 25 vol.% of CC1 (curve 1), CC2 (curve 2) and CC3 (curve 3). Curves were constructed by subtraction of normalized melting curve of plain HDPE from normalized melting curves of the blends.

i.e. a thickness increase should be expected for the lamellae. Thus, the population of the thin crystallites in the blend is most likely present in the near-interface regions where the HDPE–CC interface was able to directly influence the crystallization process and modify the number density and size of lamellar crystallites.

3.3. Tensile properties

Table 3 presents the results of tensile tests performed at room temperature at a deformation rate of 50 mm/min (initial strain rate of 0.0167 s^{-1}). Fig. 3 shows representative nominal stress–strain curves (load–extension curves) obtained for HDPE/CC2 blends. The data shown in Table 3 demonstrate that Young's modulus increases in the blends with increasing concentration of CC filler, while the yield stress gradually decreases with increasing CC content. Comparison of moduli of blends with different CC fillers shows that the filler with large particles (CC1) causes a slightly stronger increase of the modulus than those with smaller particle size (CC2 or CC3). This filler also causes a somewhat stronger depression of the yield stress. However, the variation of both modulus and yield stress with the size of the particles is small and the mechanical response is controlled primarily by the volume fraction of the filler rather than by its particle size. The flow stress shows a similar trend to the yield stress, i.e. decreasing slowly with increasing filler content, but a variation that is smaller than that in the yield stress (see Fig. 3). A comparison of ultimate elongation of the blends and neat HDPE demonstrates that fillers induce a definite decrease in elongation to fracture which becomes very substantial for some samples with large CC volume fraction, where fracture occurs shortly after yield. This is most aggravated in the blends modified with large particles of CC1.

Visual observation of deforming specimens of particle-modified HDPE showed that yield and plastic flow is accompanied by very strong whitening of the blend in the

Table 3
Tensile properties of HDPE/CC blends at room temperature and the initial deformation rate of 1.67×10^{-2} s^{-1}

Blend code	Volumetric composition (PECC)	Young's modulus (MPa)	Yield stress (MPa)	Yield strain (%)	Stress at break[a] (MPa)	Elongation at break (%)
HDPE (control)	100:0	756.1	24.9	11.5	14.5	730
HDPE/CC1	90:10	896.8	21.9	10.3		319
	80:20	1235.0	19.6	7.6		36
	75:25	1274.1	18.8	7.8	11.7	64
	70:30	1806.4	15.6	3.3	11.8	10
HDPE/CC2	95:5	818.2	23.8	10.5	13.8	696
	90:10	961.9	22.9	9.1	13.5	200
	85:15	1136.5	21.3	7.5		37
	80:20	1209.8	20.2	6.3		33
	75:25	1207.8	20.0	5.6	13.8	205
	70:30	1604.8	19.2	—	19.2	5
HDPE/CC3	75:25	1197.90	20.45	11.50	10.50	186

[a]Fracture load divided by initial cross-sectional area

necking zone for all fillers and compositions studied. This suggested extensive debonding of the particles from the matrix occurring near the yield point confirms a state of low adhesion between components, where apparently surface treatment with calcium stearate does not improve adhesion but merely serves the purpose of random dispersal of particles. Fig. 4 presents a typical SEM micrograph of a stretched tensile specimen of the HDPE/CC1 (75:25) blend. Elongated cavities are clearly visible around debonded filler particles. Final fracture of the sample is initiated by some interior imperfection of the structure such as a large filler particle or agglomerate in the specimen encountered by the propagating neck. A crack that forms starts to propagate initially stably away from the local source. Due to the chance encounter of the propagating neck with such an imperfection, ultimate elongations of the specimens of the same composition frequently varied widely. A particular

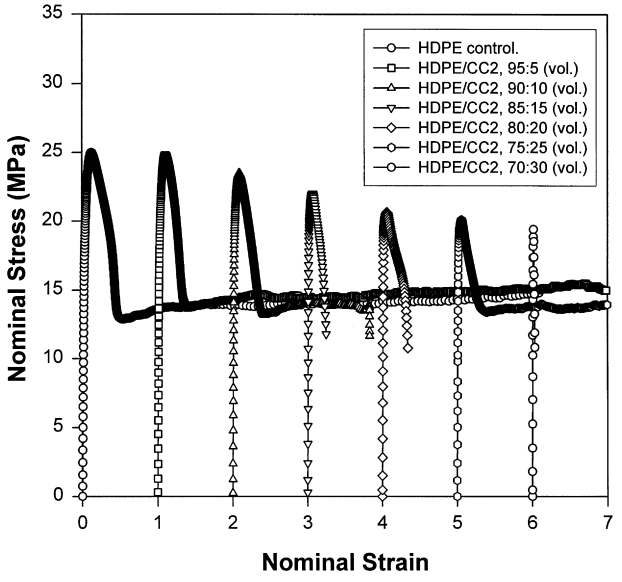

Fig. 3. The stress–strain (load–extension) curves of the series of HDPE/CC2 blends with volume compositions varying from 100:0 (plain HDPE) to 70:30. For clarity each curve was shifted along the strain axis.

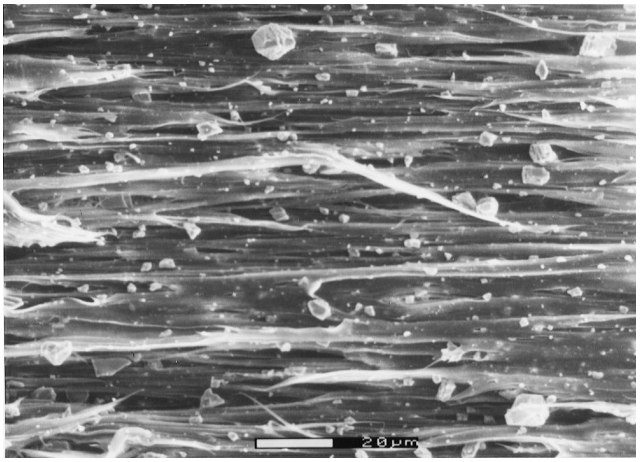

Fig. 4. SEM micrograph of the HDPE/CC1 (75:25, vol.) tensile specimen within the stress-whitened neck zone.

example of this behaviour was observed in the specimens of HDPE/CC2 of 75:25 composition coming from two nominally identical batches, both processed under the same conditions. While the specimens from one batch deformed easily to an elongation of more than 300%, most of those from the second batch failed at elongations of less than 30%.

These changes in the tensile behaviour of filled HDPE are similar to those reported previously by other investigators in blends of polyolefins with mineral fillers in which the adhesion of the components was not enhanced by any special treatment.

3.4. Izod impact response

Fig. 5 shows the notched Izod impact energies, I_s, measured at room temperature in samples of neat HDPE and HDPE/CC blends containing 25 vol.% of various CC fillers. The data for specimens cut out from the *gate end* and the *far end* of the flexural bars[2] are reported separately for each

[2] A detailed description of the terminology of '*gate end*' and '*far end*' of injection-moulded samples is given in (I)[11].

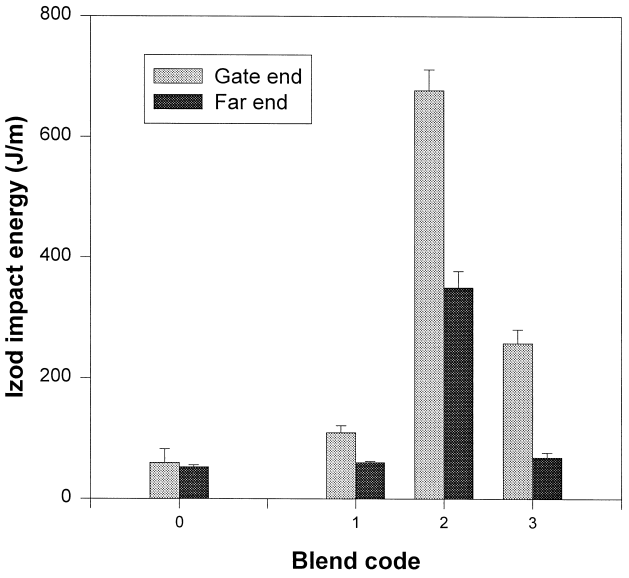

Fig. 5. Notched Izod impact energies measured at room temperature for samples of plain HDPE (code 0), HDPE/CC1 (code 1), HDPE/CC2 (code 2) and HDPE/CC3 blend (code 3). All three blends contain 25 vol.% of calcium carbonate. Data for *gate end* specimens and *far end* specimens shown separately.

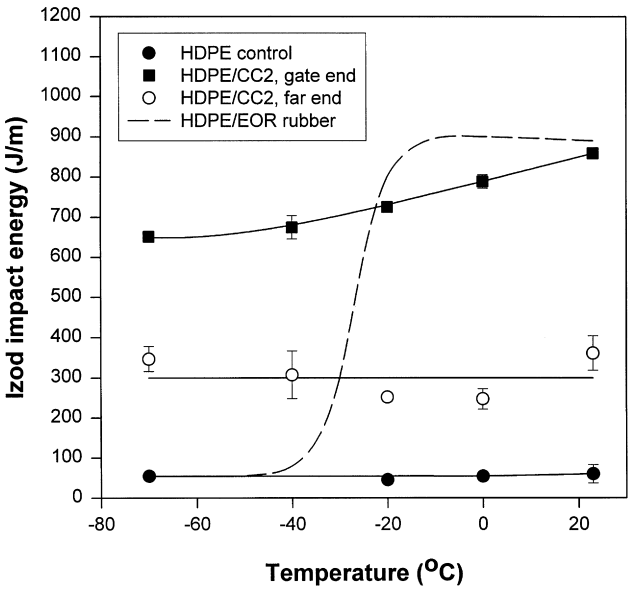

Fig. 6. The dependence of notched Izod impact energy on temperature for the HDPE/CC2 blend. For comparison the curves determined for blends of HDPE with EOR rubbers 78:22 (vol.) (taken from Ref. [11]) are also presented (dashed line).

composition. The values obtained for the specimens from the *gate* and *far ends* are similar in the case of neat HDPE, but differ substantially in blend samples. These differences of toughness of *gate* and *far end* specimens result, most probably, from different microstructural orientations produced in these parts of the bar by the flow of the charge in the mould during the injection-moulding process, as will be discussed below. Nevertheless, if discussion is restricted to only the data obtained from the *far end* specimens (exhibiting lower values of I_s) it can be observed that modification of HDPE with 25 vol.% of CC particles leads to some improvement in toughness for every filler type used. Such modification increases the impact energy of the polyethylene in all three blends, but this increase depends strongly on the size of CC particles. While modification with CC1 filler particles of number-averaged size $\langle d_n \rangle = 0.85\ \mu$m; increases I_s by merely 20% compared to neat HDPE, modification with CC2 particles with $\langle d_n \rangle = 0.41\ \mu$m causes a huge increase of I_s by more than 700%. Modification with CC3 particles of $\langle d_n \rangle = 0.15\ \mu$m results in only 30% increase in I_s as compared to neat HDPE for reasons of poor particle dispersion. The same trends can also be observed for specimens cut from the *gate end* of the injection moulded bars, although the improvement of the toughness of the blends in this group of specimens is far more impressive than those observed for the *far end* specimens. Samples of HDPE/CC2 had impact energies approximately 12 times higher than those of neat HDPE (in the best instance a 15-fold improvement occurred for one batch of HDPE/CC2 (75:25) blend!).

The samples of the neat HDPE and HDPE/CC1 blend broke nearly completely during the test (partial break according to the definition of ASTM D-256), while those of HDPE/CC2 did not break completely (30–50% of the cross-section remaining unbroken) and bent instead to allow the pendulum to swing by. The specimens of HDPE/CC3 blend demonstrated mixed behaviour: those taken from the *far end* of the flexural bar usually broke partially and those from the *gate end* did not break, similar to the HDPE/CC2 samples. Comparative examination of the samples after the test revealed that neat HDPE did not whiten, HDPE/CC1 were whitened on the fracture surface, whereas in HDPE/CC2 and HDPE/CC3 the stress-whitened zone developed beneath the crack flanks and ahead of the crack tip. This zone was especially large in the samples of HDPE/CC2, where it extended to a depth of nearly 2 mm away from the crack flanks.

The dependence of Izod impact energy of the blends on temperature was also investigated. Fig. 6 summarizes the results of these studies obtained for the HDPE/CC2 blend. The other blends, not shown in this Figure, demonstrated similar behaviour, albeit in ranges of considerably lower impact energy. In this figure the dependence on temperature of I_s of HDPE modified with EOR rubber reproduced from (I)[11] is also shown for the purpose of comparison with the results of the present study. The shape of the curves obtained for HDPE/CC blends demonstrate only a very weak dependence of impact energy on temperature within the temperature range studied. Examination of the samples tested at various temperatures showed similar impact behaviour at all temperatures with generation of stress-whitened zones of similar size. These observations show that the toughness of the system depends only on the matrix properties, while the interactions of the matrix and the filler

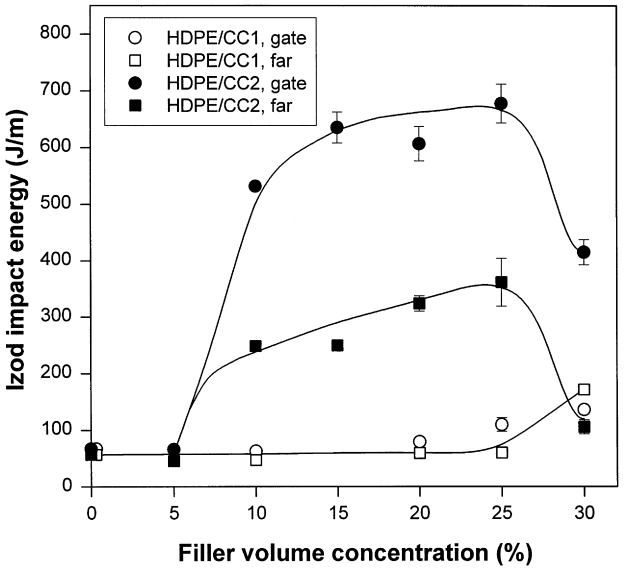

Fig. 7. The dependence of notched Izod impact energy on the concentration of the filler, determined for the samples of HDPE/CC1 and HDPE/CC2 blends. The data for specimens from *gate end* and *far end* are shown separately.

particles seem not to change with decreasing temperature. This behaviour is strikingly different from that which was found for rubber-modified HDPE (and other rubber-modified polymers as well), in which high toughness is limited only to temperatures above T_g of the well-bonded rubber inclusions, which in the EOR rubber modified HDPE blends is in the range of −15 to −30°C, making these blends brittle at lower temperatures [11]. Therefore, for polymers with matrixes having amorphous components of low glass transition temperatures toughening with stiff fillers has clear advantages over rubber modification[3].

Fig. 7 presents the Izod impact energy at room temperature of the HDPE/CC1 and HDPE/CC2 blends as a function of their composition. It can be seen that in the case of the HDPE/CC2 blend there is a strong jump of impact energy occurring at the filler concentration between 5 and 10 vol.%. Further increases of filler concentration causes only slight improvement of the impact energy. For CC2 concentrations approaching 30%, a substantial decrease of impact energy develops. These trends can be observed for both the *gate end* and *far end* specimens, albeit as before, the changes are much stronger in the *gate end* specimens. In the case of HDPE/CC1 blend the impact energy remains nearly constant and on the low level, characteristic of neat HDPE up to concentrations of 25 vol.%, with a slow rise observable at concentrations higher than 30 vol.%. As we will discuss later, the increase of the impact energy in both samples of HDPE/CC1 and HDPE/CC2 is accompanied by changes in

[3] Parenthetically, in the model of toughening studied here there is no evidence that a glass transition in the amorphous component of the semicrystalline matrix will have any deleterious effect. The mechanism of the deleterious effect of the glass transition in the rubbers of the rubber-modified material is quite different and was explained in (I)[11].

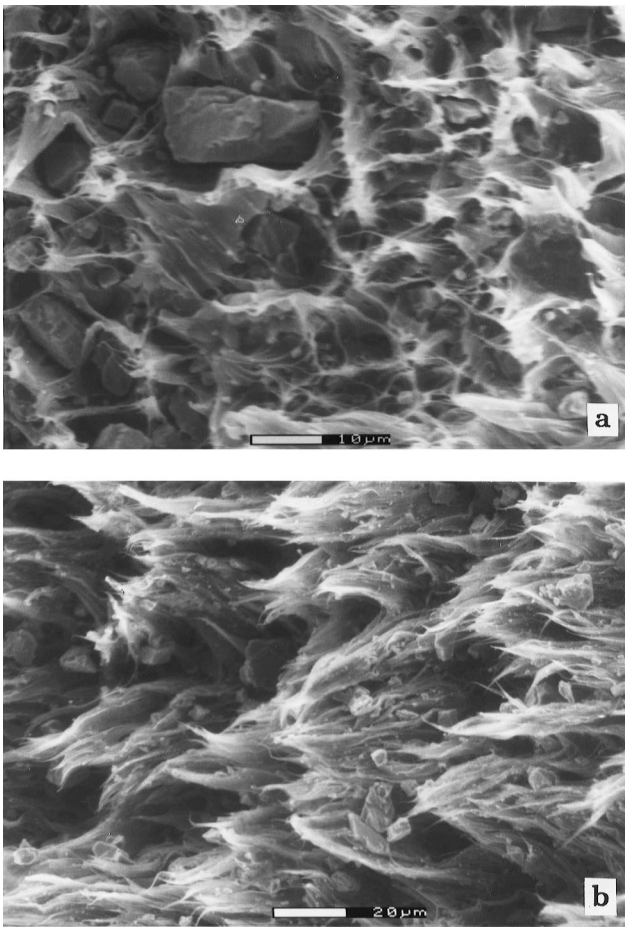

Fig. 8. SEM micrographs of the fracture. surface of Izod samples of HDPE/CC1 blend: (a) 75:25 (vol.%), (b) 70:30 (vol.%). The direction of crack propagation was from right to left. Note different magnification of micrographs; scale bar shown on every micrograph.

the fracture mode from brittle to tough so that an increase of I_s, observed at 30 vol.% of CC1, most probably indicates the beginning of the toughness jump similar to that observed below the 10% concentration level in the HDPE/CC2 blend. However, preparation of samples with unclustered filler concentrations higher than 30 vol.% is much more difficult to achieve. Therefore, this range of behaviour was not explored.

3.5. Morphology of fracture surfaces and plastic deformation zones

Figs 8–10 show SEM micrographs of fracture surfaces of samples of the HDPE/CC1, HDPE/CC2 and HDPE/CC3 blends, respectively. The micrographs in Fig. 9 demonstrate that in the HDPE/CC2 samples with 0.05 vol. fraction of particles the fracture is semi-brittle with very little plastic deformation of the HDPE matrix observable on the fracture surface. This composition showed impact energies comparable to neat HDPE (recall Fig. 7). In contrast, fracture surfaces of samples of HDPE/CC2 blends with 0.1–0.25 vol. fraction of particles, exhibiting high impact energy, show

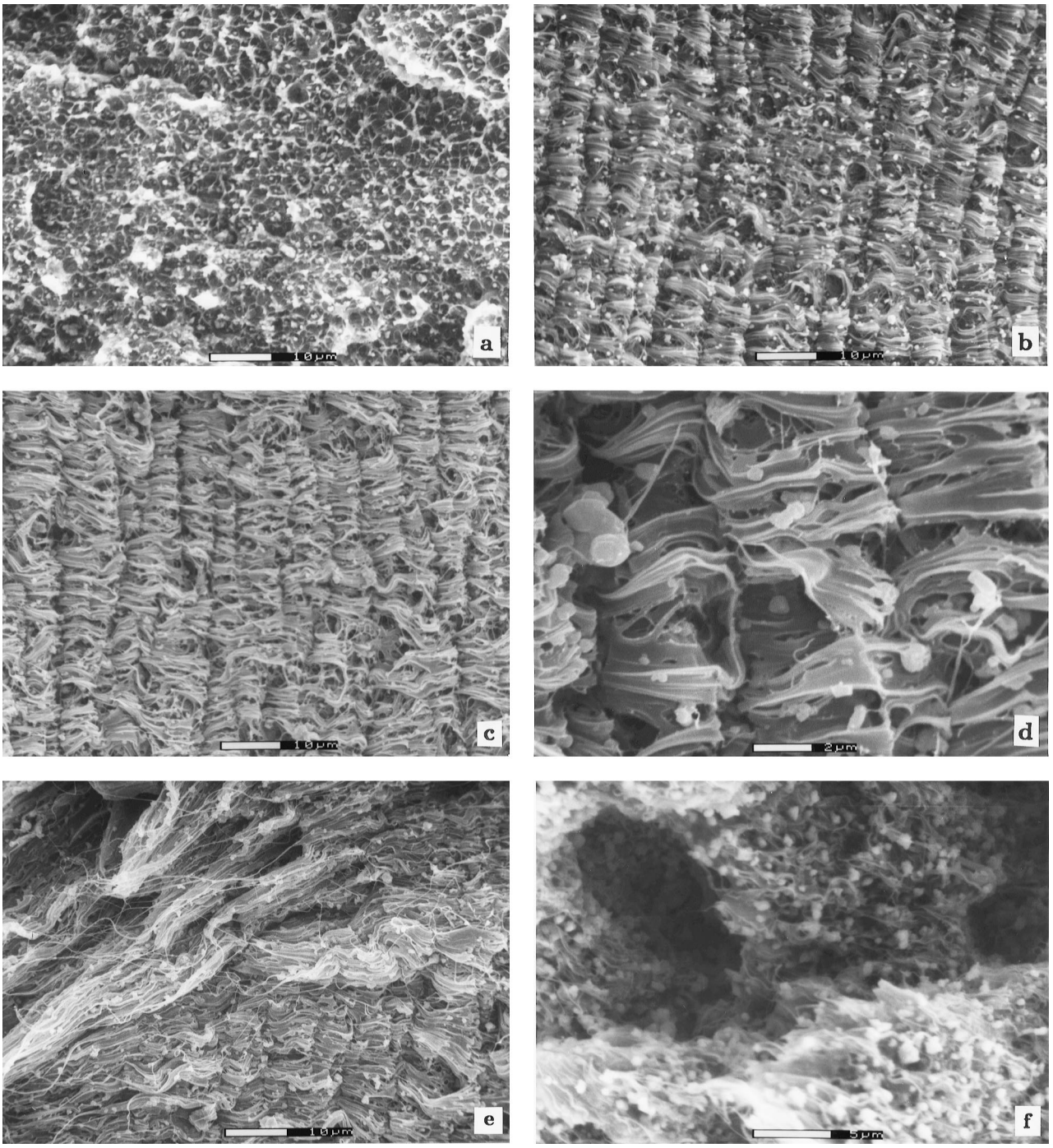

Fig. 9. SEM micrographs of the fracture surface of Izod samples of HDPE/CC2 blend: (a) 95:5 (vol.%), (b) 90:10, (c) 75:25, (d) the same as (c) under higher magnification, (e) 75:25, different location, (f) 70:30. The direction of crack propagation was from right to left. Note different magnification of micrographs; scale bar shown on every micrograph.

extensive plastic deformation of the matrix accompanying crack propagation. In this range of CC2 concentration, a characteristic feature of the fracture surface is the formation of regular striations perpendicular to the direction of crack propagation. In (I) [11] formation of similar striations in the HDPE/rubber blends was reported. Such striations were observed earlier in rubber-modified Nylon 6,6 where their origin as surface folds was explained fully [13]. Fig. 9d shows a more detailed view of that morphology, observed at larger magnification. This micrograph shows that these striations are associated with heavily plastically deformed fibrils of the HDPE between particles of CC2. Fig. 9e shows a somewhat different type of morphology observed in these samples. In the lower right part of the micrograph the same striations can be seen, which gradually transform into more elongated rough structures as seen in the upper left part of

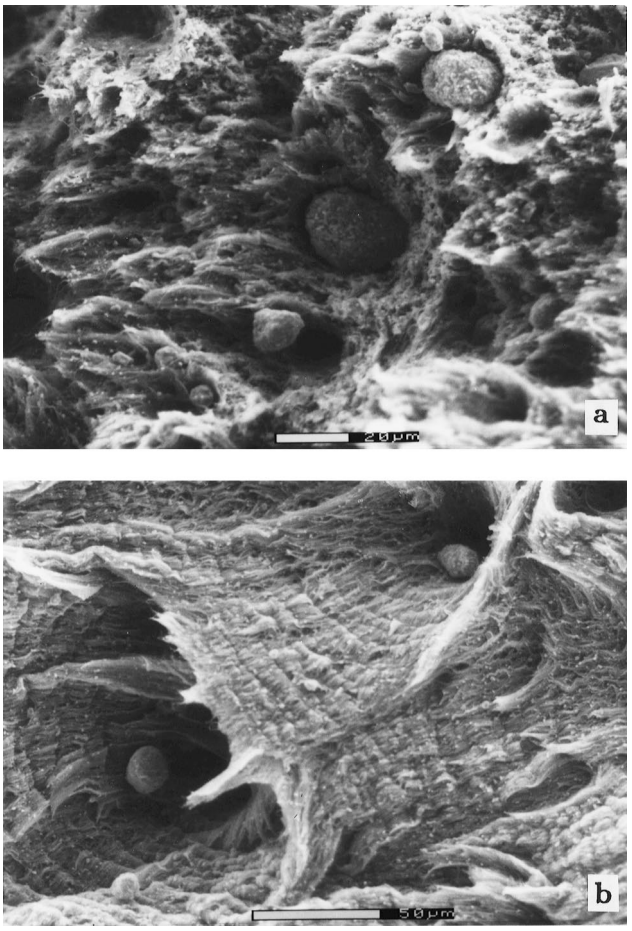

Fig. 10. SEM micrographs of the fracture surface of Izod samples of HDPE/CC3 blend 75:25, (a) and (b) taken at different location of the same surface. Note different magnification of micrographs; scale bar shown on every micrograph.

the micrograph. When observed at lower magnification these also reveal a periodicity similar to the more compact striations reported above, so that they must represent the same striation-type morphology, which, however, must have formed at somewhat different deformation conditions. A characteristic feature of these longer and more irregular striations is the extremely long filaments indicating very large strain plastic deformation of the matrix—accompanying the local fracture process. These rough, longer striations can be found near the centre line of the fracture surface and considerably away from the notch, while the compact striations with shorter periods (typical of those in Fig. 9c,d) were found on the sides of the fracture surface and close to the notch. Formation of such striations was studied in detail by Muratoglu et. al. [17], who found that the change from compact to rough morphology, accompanied by an increase of the striation period, occurs with a decrease of crack velocity and/or increase of temperature. On the basis of these observations we conclude that some adiabatic heating of the sample must have occurred during the high-speed Izod impact tests of HDPE/CC2 blends, which resulted in the changes of the striation morphology between the centre of the sample and regions near the notch. The presence of highly elongated thin fibrils in these regions is in support of the above conclusion, since such large elongations are possible only at elevated temperatures.

Fig. 9f demonstrates that the character of the fracture in the HDPE/CC2 blend changes again at CC concentrations of 0.3. The fracture surface in that specimen showed much less plastic deformation than in samples of lower CC2 concentrations. Additionally, relatively large clusters of CC2 particles appear on the fracture surface. This clearly demonstrated that the dispersion of the filler particles becomes much worse with higher filler concentrations, compared with blends of lower filler concentrations. Evidently, the presence of these clusters or agglomerates was responsible for the earlier fracture of the sample and the low impact energy (cf. Fig. 7).

Fig. 8a,b illustrates the morphology of the fracture surface of the HDPE/CC1 blend with larger mean particle size. Fig. 8a shows the fracture of the HDPE/CC1 (75:25) blend sample, while Fig. 8b that of the HDPE/CC1 (70:30) blend. Fig. 8a shows that there are traces of plastic deformation limited to the fracture surface of the blend containing 0.25 vol. fraction of the CC1 filler, while Fig. 8b illustrates that for the CC1 concentration of 0.3 the fracture was accompanied by extensive plastic deformation, and features similar to the striations observed in the HDPE/CC2 samples can be clearly seen in this sample. Again, as in the case of HDPE/CC2 blend, the changes of the fracture surface morphology of HDPE/CC1 blend shows good correlation of the measured large impact energy and extensive plastic deformation in the tough samples. It is noteworthy that dispersion of particles in the HDPE/CC1 (70:30) blend appears good, in comparison to the HDPE/CC2 (70:30) blend discussed above. However, the CC1 blend had much larger average particle size, which meant that the average interparticle ligament thickness in this blend was considerably larger than in the blend containing 0.3 of CC2.

Fig. 10 presents micrographs of the fracture surface of the Izod samples of HDPE/CC3 (75:25) blend. We recall, that this blend exhibits impact energy only slightly higher than that of neat HDPE, and much lower than the HDPE/CC2 blend of the same volume composition (cf. Fig. 5). That the poor performance of this blend is different from the latter blend could not be expected on the basis of the particle size alone, since the smaller the particle size at this concentration the more effective the toughening should be, analogous to the modification with rubber. However, as already discussed, this filler had a much broader size distribution of particles compared with the CC2 blend, and additionally contained a fraction of large, stable aggregates, since it could not be surface-modified (cf. Table 1 and Fig. 1c). Moreover, the large aggregates apparently had survived break-up during processing and remained present in the blend, resulting in a profoundly deleterious effect on the performance of the blend. Fig. 10a,b shows that these aggregates induce premature fracture in the HDPE/CC3 (75:25)

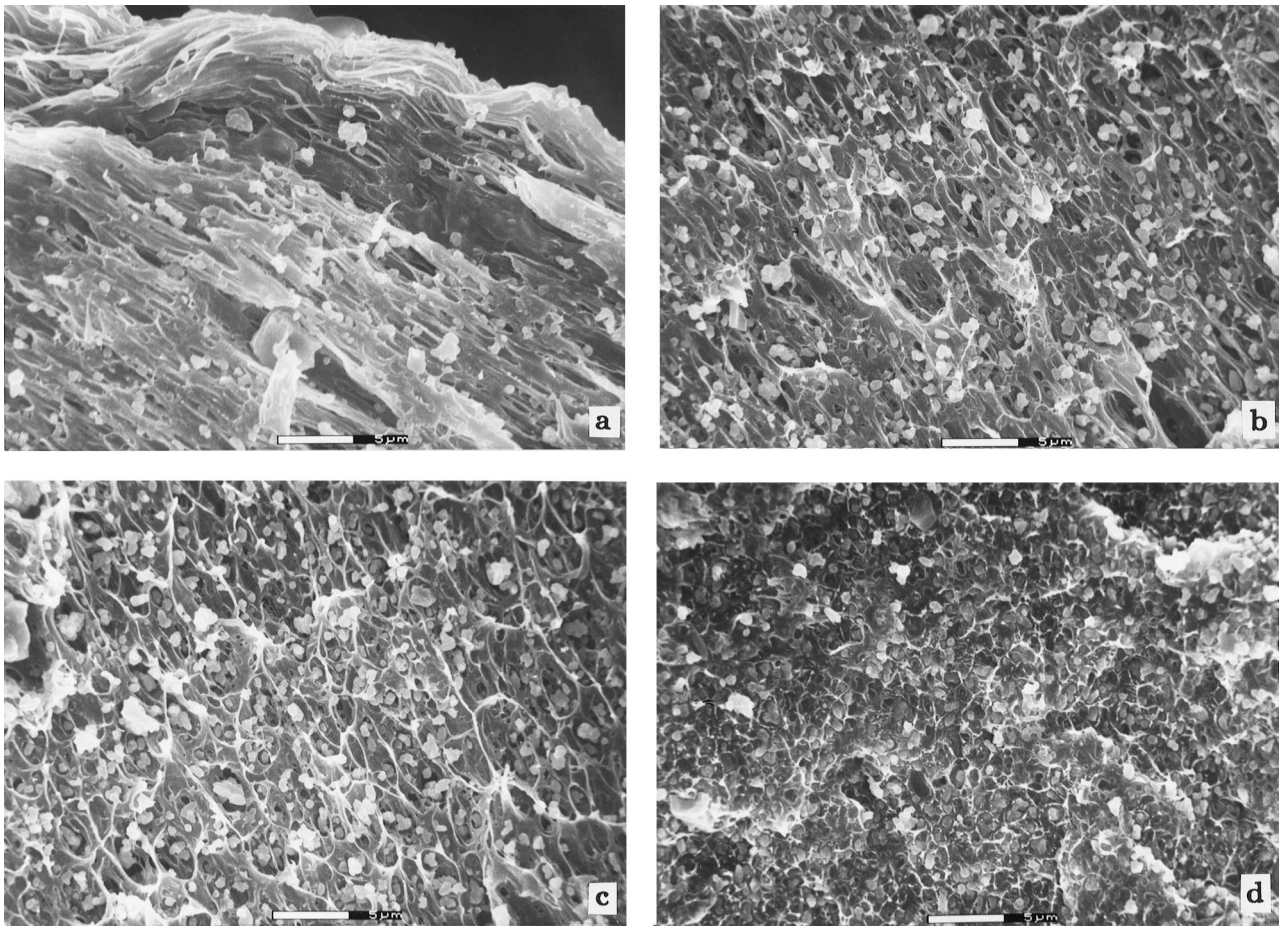

Fig. 11. SEM micrographs of the sample of HDPE/CC2 75:25 (vol.%) cryofractured along the symmetry plane of the sample perpendicular to the fracture plane (IZOD1 view; for details see Ref. [11]). Location of the micrographs are: (a) directly under crack flank, (b) 160 μm under crack flank, (c) 520 μm under crack flank, (d) 980 μm under crack flank. The direction of crack propagation was from right to left. Scale bar represents 5 μm.

blend in the impact test, frequently becoming sources of the secondary cracks, as Fig. 10b shows. Once initiated by such agglomerates the secondary crack extends radially outwards with the formation of striations characteristic of the tough HDPE/CC2 blends. However, the number density of such secondary crack sites induced by the agglomerates on the fracture surface is so large that the net result is a low impact energy of the material, in spite of tough superficial behaviour demonstrated around such sites. Fig. 10 demonstrates clearly that the CC3 filler has a great potential for toughening HDPE, which, however, remains largely neutralized by the excessive agglomeration. If effective surface modification for this filler can be used to achieve more uniform dispersion very effective toughening may indeed result.

Additional investigations of the toughening mechanism in the presence of CC particles were performed by means of SEM observations of the morphology of the stress-whitened plastic deformation zone developed near the crack flanks during crack propagation. For this, representative Izod samples of the tough HDPE/CC2 (75:25) blends were cryofractured after the impact test in two perpendicular sampling planes, both perpendicular to the fracture surface. Figs 11 and 12 present the SEM micrographs recorded at various locations within the plastic deformation zone, in the cryofractured IZOD1 and IZOD2 planes, respectively[4].

In both planes the extensive cavitation associated with debonding of the filler particles from the matrix can be seen. As demonstrated in tensile experiments, debonding occurs at or before yielding of the HDPE matrix, starting at the polar regions of the particles, and resulting in elongated cavities as the matrix undergoes plastic extension. The long axis of such cavities coincides with the principal direction of tensile extension, and their length and orientation furnish good measures of the local extension ratios as well as the principal direction of the local stretch. In Figs 11 and 12 very similar cavities can be seen in the plastic deformation zone of the Izod samples. Evidently, these cavities are the source of the whitening of the material in the plastic deformation zone. Fig. 12, presenting the IZOD2 view, reveals that the cavities have a roughly circular cross-section (the long axes of cavities being oriented in the IZOD1 plane, perpendicular to the IZOD2 plane, accounting for the shape of the sectioned cavities on the IZOD2

[4] A description of these sampling planes, labelled as IZOD1 and IZOD2 is given in (I)[11].

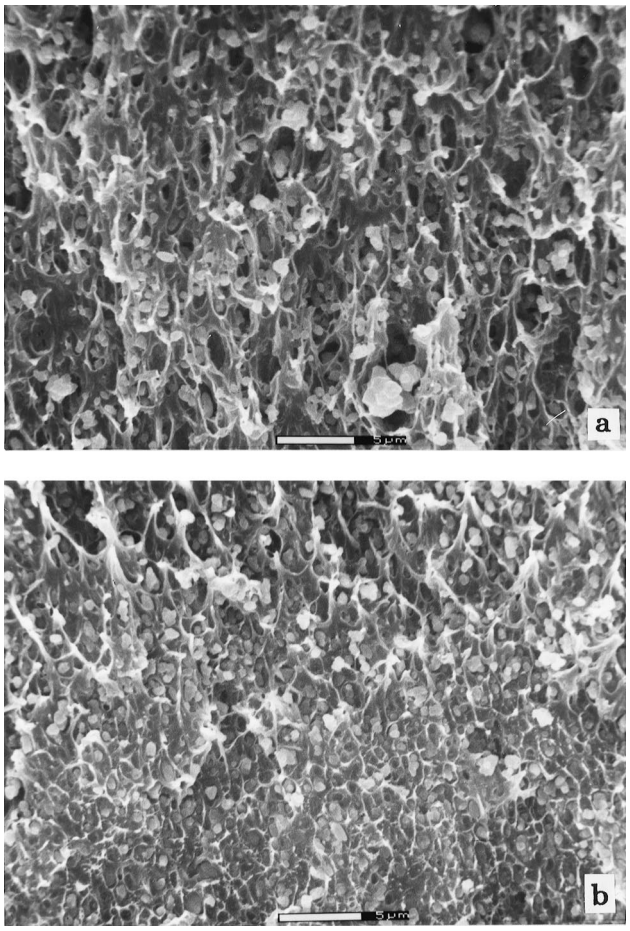

Fig. 12. SEM micrographs of the sample of HDPE/CC2 (75:25, vol.%) cryofractured along the plane perpendicular to fracture plane and symmetry plane of the sample (IZOD2 view; for details seeRef. [11]). Location of the micrographs: (a) directly under crack flank, (b) close to the end of stress-whitened zone (ca. 1.5 mm from fracture surface). Scale bar represents 5 μm.

plane). The micrographs presented in Fig. 11a–d, taken at locations with increasing distance from the crack flank demonstrate that the length of the cavities and their orientation changes gradually with distance from the crack flank. Right below the fracture surface the cavities are very long, with an aspect ratio of approximately 8–9 and oriented nearly parallel to the fracture plane (Fig. 11a). The cavities located directly under the fracture plane even follow the waviness of the fracture surface folds, and give another view of the striations on the fracture surface (Fig. 8b–e). The cavities located 10–20 μm below the crack flank are somewhat shorter than those directly beneath the flank and are oriented with their long axes at a small angle with respect to the fracture plane. The length of the cavities gradually decreases and their orientation angle increases with increasing distance from the crack flank (see Fig. 11b–d). Near the end of the deformation zone they are merely equi-axed and slightly larger than the particles from which they have formed by debonding. The changing shape and tilting of the principal axes of the elongated cavities and the kinematical processes of deformation near the tip of a propagating crack that have led to this development have been discussed in detail by Muratoglu et al. [17] in Nylon 66/rubber blends. All morphological features reported here for the HDPE/CC blends are in full agreement with that explanation.

The fracture process morphology of the deformation zone in the present study is the same in every detail as that reported in the HDPE/rubber blends of (I) [11]. The important difference is that the cavities in the HDPE–rubber blends resulted from internal cavitation of rubber particles while in the present study they result from debonding of the particle from the matrix due to the interfacial stress concentrations accompanying yielding. The very close resemblance of the final morphologies of the deformation zone indicate that the large increase of toughness observed in both rubber- and CC-modified HDPE must originate from the same mechanism of deformation of oriented crystalline layers where the action occurs in both systems. The specific mechanism of cavity formation is of lesser importance, provided that it occurs to permit unconstrained plastic stretch of interparticle matrix ligaments.

3.6. Processing-related material orientation

As was stated above, in the toughness investigation two sets of specimens were used coming from two ends of the injection-moulded specimen blanks. The bars from which the Izod specimens were produced were formed by injection of molten charge into the moulds equipped with a single filling gate located axially at one end of the mould. The injected bars were divided into two equal size pieces and were machine-notched to obtain the specimens for the Izod impact tests. The part closer to the gate was labelled as *gate-end* while the distant end was labelled as *far end*. For every composition studied, including neat HDPE, the impact energy measured in the specimens from the *gate ends* of the flexural bars was higher than in those from the *far ends*. It is known that parts formed by injection moulding frequently exhibit an orientation induced by flow of the polymer in the mould [18]. Such possible orientation could induce some changes in toughness of the material as measured by the Izod impact test. The effect, while negligibly small in neat HDPE, intensifies markedly in the blends. Similar important effects of such flow orientation on impact energy was also observed in HDPE/rubber blends, reported in (I) [11], where, however, differences were not as large as those found in the present study of HDPE/CC blends.

In order to ascertain the extent of this orientation and its role on improvement of toughness, the orientation in the *gate end* and *far end* of Izod specimens was studied by X-ray diffraction. These are discussed in Appendix A and demonstrate that, while the measurable orientations are minor, their effects on the toughness properties are not negligible. They indicate that such processing variables

may have important practical applications in the development of industrial products.

4. Discussion

4.1. Application of the criterion of toughening to HDPE/CC blends

Based on the already-reported similarities between deformation behaviour of the HDPE toughened with rubber and calcium carbonate particles, we demonstrate the unity of mechanisms involved through the critical ligament thickness criterion of Wu [12] in the blends studied here. According to this criterion a polymer modified by rubber particles shows a transition from brittle to tough behaviour when the thickness Λ of the interparticle matrix ligaments decreases below a critical value Λ_c, which is specific for that polymer [11]. The criterion emphasizes the primary role of the matrix in the toughening mechanism, and relegates the exact properties of the particles to minor importance. We start by noting that in our more narrow interpretation, the criterion of Wu requires a semi-crystalline morphology and should not be applicable to other morphologies where crystal plasticity plays no role. Wu's criterion has been given a much wider interpretation, particularly in glassy polymers, nearly always without much mechanistic justification (see our discussion in the companion study [15]).

The matrix ligament thickness Λ in the blend relevant in Wu's criterion can be estimated using the following equation [11,12]:

$$\Lambda = d \times [\beta(\pi/6\phi)^{1/3} - 1] \times \exp[(\ln \sigma)^2] \quad (1)$$

where, d, is the number average geometrical mean diameter of particles, β is a geometric constant, depending on the assumed packing of the particles (1.0 for a cubic lattice, 1.09 for body-centred cubic and 1.12 for face-centred cubic packing[5]; β is taken as 1 here [12]), ϕ is the volume fraction of the particles and σ is the geometrical standard deviation of the particle size distribution.

Eq. (1) was used to calculate the interparticle ligament thickness for the blends of HDPE with CC1 and CC2 at various compositions. The characteristic parameters d and σ for CC1 and CC2 fillers were taken from Table 1. The calculated values of Λ were used instead of the composition to replot the data of Fig. 7. The resulting dependence of Izod impact energy on ligament thickness Λ is shown in Fig. 15. Clearly, in this form of unified representation the impact toughness does not depend directly either on the blend composition or the particle size, and offers a direct comparison of the effectiveness of all blends. This plot demonstrates that for large ligament thickness the toughness of both blends of HDPE/CC1 and HDPE/CC2 remains low and at the same level characteristic for neat HDPE, until the ligament thickness decreases below approximately 0.6 μm. Near this value of $\Lambda = \Lambda_c$ a sharp upward jump in the impact energy occurs in both blends and in both the *gate end* and *far end* specimen types. For comparison the 'master curve' obtained for the blends of HDPE with 11 various rubbers investigated in (I) [11] is also plotted as the solid curve. Remarkably, both data sets for HDPE/rubber and HDPE/CC blends follow the same behaviour envelope. The only difference is that the toughness for HDPE/CC blends branch out from this 'master curve' on its high toughness side at a lower level than for the HDPE /rubber blends. The reason for this is not entirely clear.

4.2. The toughening mechanism

In the accompanying related study (III) [15] we have investigated the details of crystallization of polyethylene in the near-interface zone in model thin films of HDPE crystallized against both amorphous rubber and crystalline (calcite) substrates. Our findings demonstrate that crystallization habits of PE near an incoherent interface are much different from that which occurs in bulk. Essentially the same crystallization behaviour of PE was found in the presence of HDPE/rubber interfaces as well as HDPE/calcite crystal interfaces. Probing the near-interface morphology of the HDPE crystallized from the molten state, with WAXS and atomic force microscopy (AFM), we demonstrated that PE crystallizes preferentially in these interfacial layers with the lamella oriented edge-on against the substrate and with a strong preferred orientation of the crystallographic (100) planes lying parallel to the interface. The branching and twisting of lamellae are strongly suppressed in the near-interface layer, and bunched up lamellar crystallites grow in the form of nearly straight ribbons around the interface plane. It was found that such a layer of the oriented growth has a thickness of up to 0.4 μm. In films with larger thickness, while the oriented near-interface layer appears to remain unaltered, the overall morphology gradually transforms into a random arrangement, characteristic for bulk material as the interior of the film fills up with lamellae of random orientation. It must be emphasized that the crystallization of HDPE in contact with amorphous rubber and calcite monocrystals was found to proceed in substantially the same way in all cases where (100) planes, containing the chain axis, align parallel to the substrate, with, however, no preferred orientation of chain axis existing within this plane over the entire population of lamellae. This demonstrates that such oriented special forms of crystallization of HDPE are induced by the presence of the incoherent interface itself, independent of the nature of the substrate, whether that be amorphous (liquid) or crystalline. Even in the case of crystalline calcite substrates, the crystallization habits were found to be the same and have no epitaxial character. Similar oriented crystallization behaviour was also found earlier in Nylon 6 when crystallized against Nylon–rubber

[5] These values differ from those reported by Wu who appears to have considered incorrect geometry.

interfaces [14]. This suggests that this type of crystallization near incoherent interfaces is quite common in semi-crystalline polymers for a broad variety of interface types, including liquid–liquid and liquid–crystalline solid interfaces.

A calcite monocrystal was used as a substrate in our above-mentioned studies as a model for the calcium carbonate filler to avoid complications due to grooves around loosely packed filler particles. Therefore, it can be expected that the near-interface layers around each CC particle in the HDPE/CC blends have the same character. That this is so has confirmation from the TEM studies of Chacko et al. [18], who found oriented layers of crystalline lamellae growing radially outward from around the CC filler particles in the films of HDPE/CC blends. They reported the thickness of such oriented layers to be in the range of 0.3–0.4 μm. Their observations and estimate of the thickness of the oriented layers around CC particles agrees very well with our above-mentioned findings [15].

Thus, it can be postulated that the morphology of the HDPE/CC blend consists of filler particles surrounded by shells of specifically oriented HDPE crystallites of a characteristic thickness of approximately 0.3–0.4 μm and that the background bulk consists of crystallographically unoriented HDPE matrix. Exactly the same morphology with the same thickness of oriented layers was found in the HDPE/rubber blends discussed in (I) [11] and was postulated as the source of the toughening observed in those blends. These similarities lead us to conclude that the toughening mechanism of both systems must be the same, in spite of the radically different mechanical properties of the particles used for the modification of HDPE.

The mechanism of toughening of HDPE with both rubber particles [11] and with calcium carbonate particles of the present study was initially proposed by Muratoglu et al. for the toughening of Nylon 6,6 with rubbers [13]. This mechanism was discussed in detail in (I) [11] requiring only a brief summary here. The layer of a characteristic thickness consisting of preferentially oriented crystalline lamellae around filler particles of all types possesses reduced plastic shear resistance in the low-energy crystallographic planes containing the chain axis ((100) in HDPE, (001) in Nylon), that lie parallel to the incoherent interface. Upon cavitation or debonding of the particles in the initial stages of plastic flow, large regions around the newly formed cavities, between the equatorial belt and the poles (relative to the principal axis of stretch), can undergo large shear to promote the sausage shaped extension of the cavities (as depicted in Fig. 11 of (I)—provided the plastic flow of the material outside the oriented crystalline layer does not offer too high a plastic resistance. The latter requirement is satisfied when the interparticle ligaments contain only the oriented crystalline layers of the two adjacent particles, i.e. when Wu's percolation criterion is met and the ligament thickness is less than the critical thickness for the specific polymer (0.6 μm for the HDPE blends and 0.3 μm for the Nylon blends). Under these conditions a dramatic toughness jump results. The only additional requirement for the toughening mechanism to operate is that the particles either cavitate internally (rubbers) or debond at their interfaces (CC particles), to permit the unhindered stretch of the ligaments, at the onset of plastic response. Clearly, in this mechanism the nature and mechanical properties of the particles are irrelevant, nor are their volume fractions and sizes of much importance by themselves, beyond presenting incoherent interfaces for preferential crystallization and governing the interparticle ligament thickness as the correlation in Fig. 13 clearly demonstrates.

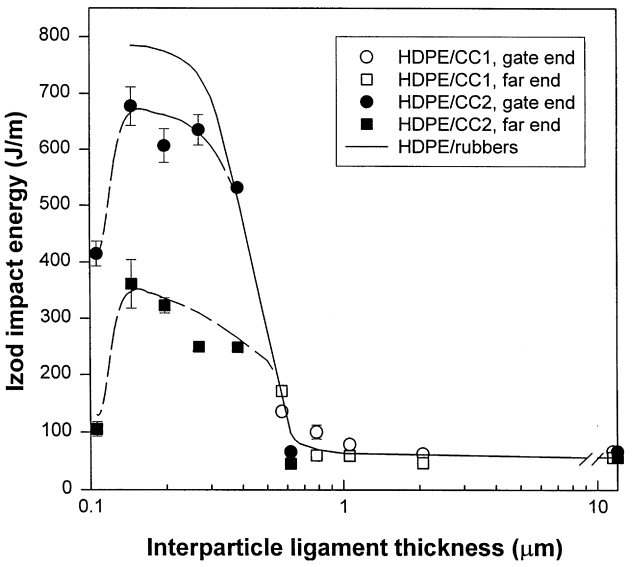

Fig. 13. The dependence of the notched Izod impact energy on the interparticle matrix ligament thickness for samples of HDPE/CC1 and HDPE/CC2 blends. The solid line represents the curve determined for the blends of the same HDPE with various EPDM and EOR rubbers (taken from Ref. [11]).

The toughening mechanism outlined above, and demonstrated to be effective in blends of HDPE with various rubbers [11], or mineral fillers (present study), as well as in Nylon 6,6 modified with rubber particles [13,17], has a universal character and should also be effective in the toughening of isotactic polypropylene modified with EPDM rubbers [19,20], but detailed morphological studies are still required to confirm this possibility in that system.

It is useful to emphasize the cavitation or debonding requirement of the toughening mechanism under consideration. This imposes certain requirements on the state of adhesion of particles to the matrix or their internal cavitation resistance. This is demonstrated in Fig. 6 comparing the toughening effects of CC and rubber particles in HDPE blends. In the former systems the cavities arise by debonding of particles upon yielding of the matrix. In the systems with rubber particles with good grafting to achieve proper dispersion and narrow particle size distributions the adhesion of the particles to the matrix is too good. This is

of no consequence as long as the rubber particles are above their T_g, where internal cavitation occurs due to deformation induced negative pressures resulting from the large difference of elastic properties of the rubber compared to the matrix. Below the glass transition of the particles the elastic mismatch between the particles and the matrix is drastically reduced, and the deformation-induced negative pressures inside the particles become insufficient to produce internal cavitation. As a result, the matrix cannot undergo the unhindered large plastic stretches and the blend is brittle. Parenthetically, we note that there has been much discussion in the recent literature on the importance of cavitation by itself as a toughening mechanism. There are indeed some cases where cavitation of particles in epoxies has been responsible for some modest toughening, the mechanisms of these cases has been discussed in some detail by Argon [21] and its contributions through crack tip shielding have been clarified by Argon et al. [22]. Such toughening is generally of minor importance and far eclipsed by the mechanism considered here.

A very similar toughening effect in PE modified with CC particles with a toughness jump of 370% at a certain ligament thickness was recently reported by Wang and coworkers [6–10]. Surprisingly, they obtained this toughening effect using much larger CC particles (in the 6–16 μm range, and found the critical ligament thickness Λ_c = 5.2 μm, which is one order of magnitude higher than that reported in the present study. In their study, a PE of relatively high toughness with an Izod impact energy of 180–230 J/m [6–8], was used which was nearly 4 times higher than that of the HDPE used here. When a PE matrix of lower toughness of around 42–45 J/m was used in their HDPE/CC blends the modification appeared to be completely ineffective [8].

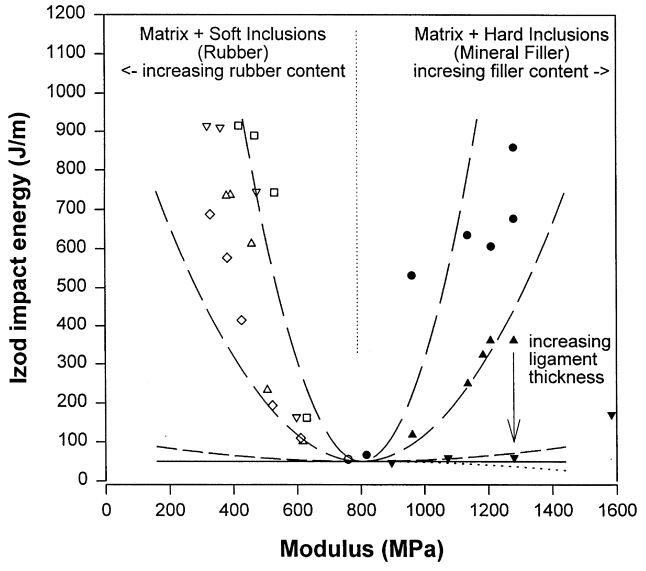

Fig. 14. Schematic plot of possible routes of toughening of semicrystalline polymers with soft particles (e.g. rubber; left branch) and hard particles (e.g. mineral filler, right branch).

We summarize our results on all the HDPE blends in Fig. 14. Homo-HDPE has a Young's modulus of 760 MPa at room temperature. Incorporation of rubbery particles with interparticle ligament dimensions below the critical threshold, results in the familiar impressive toughening effect, but at a significant compromise in the modulus by about 60%. Incorporation of CC particles at the same volume fraction and in a size range to give ligament thicknesses under the threshold value does similarly well in enhancing the Izod fracture energy, but with an added improvement of the Young's modulus by about 50%. Increasing CC particle sizes for the same volume fraction results in the same level of improvement of Young's modulus but in a drastic compromise on the toughness, since the critical ligament thickness requirement is exceeded.

The changes in the Young's modulus due to incorporation of equiaxed particles of rubber or CC with the same volume fraction are readily calculable from the work of Chow [23]. This gives the relation of;

$$\frac{E_c}{E_2} = 1 + \varphi \frac{\left(\frac{k_1}{k_2} - 1\right)\left(1 - \frac{9}{5}(1-\varphi)\right) - 2}{\left[3 - \frac{7}{5}(1-\varphi) + \left(\frac{k_1}{k_2} - 1\right)(2(1-\varphi) - \frac{14}{15}(1-\varphi)^2)\right]} \tag{2}$$

for rubbery inclusions with vanishing shear modulus relative to PE and bulk modulus ratio of k_1/k_2 between rubber (1) and PE (2) and with the Poisson's ratio of PE taken to be 1/3; and,

$$\frac{E_c}{E_2} = 1 + \frac{17}{14}\frac{\varphi}{1-\varphi} \tag{3}$$

for CC particles idealized to be rigid in both shear and bulk response relative to PE, again for a Poisson's ratio of 1/3 for the matrix PE, where subscripts (2) refer to the properties of the matrix and (1) to those of the particles. Eq. (2) gives a variation in the modulus ratio of the rubber modified PE ranging from 0.69 to 0.77 as k_1/k_2 ranges between 0 and 1.0 for a constant volume fraction of 0.22.

The experimentally observed Young's modulus ratios are in the range of 0.40 to 0.52, indicating that the incorporation of rubber must also reduce the average modulus of the PE matrix by additional morphological alterations [11]. For the case of the simpler form of Eq. (3) for the rigid CC inclusions, we estimate a 34% increase of the Young's modulus. This compares reasonably well with the observed range of 20–50% increase, where the differences could come from aspect ratios of the particles deviating from unity.

A related question to the consideration given above on the effect of rubbery and rigid particles on the elastic properties of the blends is their effect on the overall plastic resistance of the heterogeneous material. If the particles cavitate or debond upon initiation of plastic flow the question is of no

relevance. Experiments described in (I) and the results of the present study indicate that, as long as the rubbery inclusions remain above their glass transition temperatures, they cavitate readily, and the CC particles debond at apparently the inception of plastic response. If, however, this were not the case, then the above question becomes meaningful. For rubbery particles offering negligible shear resistance, the tensile resistance Y_b at yield of the rubber containing blends can be estimated from a geometrical model of Nicolais and Narkis [24] which states:

$$Y_b = Y_o(1 - 1.21\varphi^{2/3}) \tag{4}$$

where Y_o denotes the tensile plastic resistance of the unmodified matrix and φ the volume fraction of rubbery heterogeneities. For $\varphi = 0.22$ Eq. (4) gives an estimate of $Y_b/Y_o = 0.56$ which is comparable with the values observed experimentally and given in Table 2 as varying between 0.52 and 0.62.

The effect of rigid filler particles on the plastic resistance Y_b of the blend has been addressed by a number of investigators. We use the development of Huang [25] for a matrix material with a power-law stress/strain connection between the equivalent tensile plastic strain ϵ_{em} and the equivalent (von Mises) tensile stress σ_{em} of the form.

$$\epsilon_{em} = k\sigma_{em}^n \tag{5}$$

Then, according to Huang the equivalent tensile plastic resistance Y_b of the composite is related to the tensile plastic resistance of the matrix σ_{em}, at any total equivalent strain level, is:

$$\frac{Y_b(\epsilon_{em})}{\sigma_{em}(\epsilon_{em})} = \frac{(1-\varphi)}{(1-R\varphi)}\frac{1}{(1-\varphi)^{1/n}} \tag{6}$$

where φ is the volume fraction of the rigid filler and $R = R(n)$ is a numerical constant depending on the stress exponent n of the power-law connection. In both Nylon and HDPE $n \approx 3.0$, giving $R \approx 1.65$. For a volume fraction of filler of $\varphi = 0.2$, as was the case in the present study, this would result in a 29% increase of the plastic resistance of the filled polymer over the neat polymer if the CC particles did not debond. Since without debonding the special ligament plasticity could not develop, this would be highly embrittling and reinforces the commonly held view that incorporation of rigid filler into a polymer raises its stiffness but radically compromises its ductility. However, since the state of adhesion of CC particles to the HDPE matrix is quite poor, debonding of the particles does occur readily at the inception of plastic response and the special toughening processes develop fully. This emphasizes again the vital importance of ready debonding of the stiff filler particles in the course of the deformation.

Finally, it is essential to recognize that the toughness mechanism discussed in these studies involves the development of very large local plastic strains in excess of several hundreds of percent. In our earlier very extensive large strain deformation studies on both Nylon [26–28] and HDPE [29–32] we demonstrated experimentally that while these polymers contain a significant fraction of amorphous component which does indeed start off the deformation process, this component substantially 'locks-up' at strains of the order of 0.1–0.15 and that the remainder of deformation, resulting eventually in the formation of the dramatic quasi-single crystalline textures, relies almost exclusively on crystal plasticity in the lamellar crystals. Moreover, these experimental findings have been paralleled quite closely by equally extensive computational simulations based on polycrystal plasticity models [33,34] giving remarkably good agreement with the experimental findings [35]. Thus, when all the experimental evidence developed on Nylon and HDPE is considered, including the associated AFM and WAXS studies of the crystallization habits of PE in sub-micron thick layers, reported in the companion communication (III) [15], we are quite confident that the mechanisms of toughening being presented in these studies on HDPE and the earlier studies of Nylon are on very solid foundation.

Quantitative explanations of the toughening effect involving the special features of the highly elongated cavities require detailed anisotropic plasticity models which are currently being developed by Tzika et al. [36] and will be reported elsewhere.

5. Conclusions

In the present communication we report on a toughening mechanism of notch brittle HDPE, through the incorporation of calcium carbonate particles in a certain size range and volume fraction to achieve a condition of interparticle ligament dimension Λ below a critical threshold value Λ_c of 0.6 μm. Under these conditions a toughness jump is achieved which, for a volume fraction of filler of 0.22, results in Izod impact energies of 800 J/m in comparison with typical values of around 50 J/m for the neat HDPE.

Interparticle ligaments of thickness less than Λ_c possess a structure of highly ordered lamellar crystallites having reduced plastic resistance in certain orientations. When such material percolates throughout the structure the overall plastic resistance of the blend is markedly reduced and brittle behaviour is avoided. A subsidiary requirement for the toughness jump is debonding of the calcium carbonate filler particles from the matrix at yield of the matrix to permit the matrix ligaments to undergo large unhindered plastic extensions. The normal states of adhesion of the calcium carbonate particles to the matrix satisfies the debonding requirement in all instances.

Direct comparison of the experimental results of the present study with the companion study of the toughening of HDPE with rubber particles has demonstrated that the same volume fraction of calcium carbonate filler as that for rubber particles achieves the same level of toughness increase.

This indicates that the source of the toughness is the plastic extensibility of the matrix material in the interparticle ligaments and that the mechanical properties of the filler particles are of little relevance. Well-dispensed particles merely promote percolation of the preferentially ordered crystalline component of the matrix around the particles. This imparts to the mechanism a character of universality making it potentially applicable to all semicrystalline polymers where crystal plasticity plays the dominant role in large strain deformation.

While the use of calcium carbonate particles as toughness promoting agents increases the mass density of the product, they also improve the Young's modulus above that of the neat matrix and well above the reduced Young's moduli of the rubber-reinforced product. Thus, for a filler volume fraction of 0.22, while both the rubber particles and the calcium carbonate particles increase the toughness to the same degree, the former compromise the Young's modulus by 50% while the latter improve it by 50%.

Acknowledgements

This research has been supported primarily by the MRSEC Program of the National Science Foundation under award number DMR 94-00334 and has also made use of the Shared Facilities of the CMSE at M.I.T. supported under the same program. The exploratory blends were produced in the facilities of the DuPont Company under the direction of MW.

Appendix 1. Processing-related material orientation

In order to ascertain the extent of this orientation and its role on improvement of toughness the orientation in the *gate end* and *far end* of Izod specimens was studied by X-ray diffraction. The pole figures of (110) and (200) crystallographic planes of orthorhombic modification of polyethylene were determined along with the pole figure of the (104) planes of calcite in the blend specimens. These measurements revealed, in samples of neat HDPE, only minor orientation effects with the difference in minimum and maximum intensities not differing by more than ± 20% of the intensity from randomly oriented samples (the figures of neat HDPE are not shown). However, the orientation probed in the samples of the HDPE/CC2 (75:25) blend appeared stronger. These particular samples of the blend used for the determination of orientation came from the batch that had shown the largest difference between the *gate end* and *far end* (impact energies of 870 versus 360 J/m, respectively).

Fig. 15a,b presents the pole figures of the (104) plane of calcite determined in this blend from the *gate end* and *far end* specimens, respectively. It is seen that the pole figures for both specimens are essentially the same, showing concentration of the normals of the (104) planes in two arcs, the shape of which is consistent with the orientation of the crystallographic [001] axis of calcite being along the flow direction. Such orientation pattern could possibly have been produced by re-orientation of slightly elongated CC2 particles (cf. Fig. 1b) in the flow field during injection moulding. Since the intensity of the maxima are only about 1.25 times the intensity of randomly oriented material, and is practically the same in both parts of the flexural bar, the associated weak orientation most probably was not the cause of the observed toughness differences.

Fig. 16 presents the (110) and (200) pole figures deter-

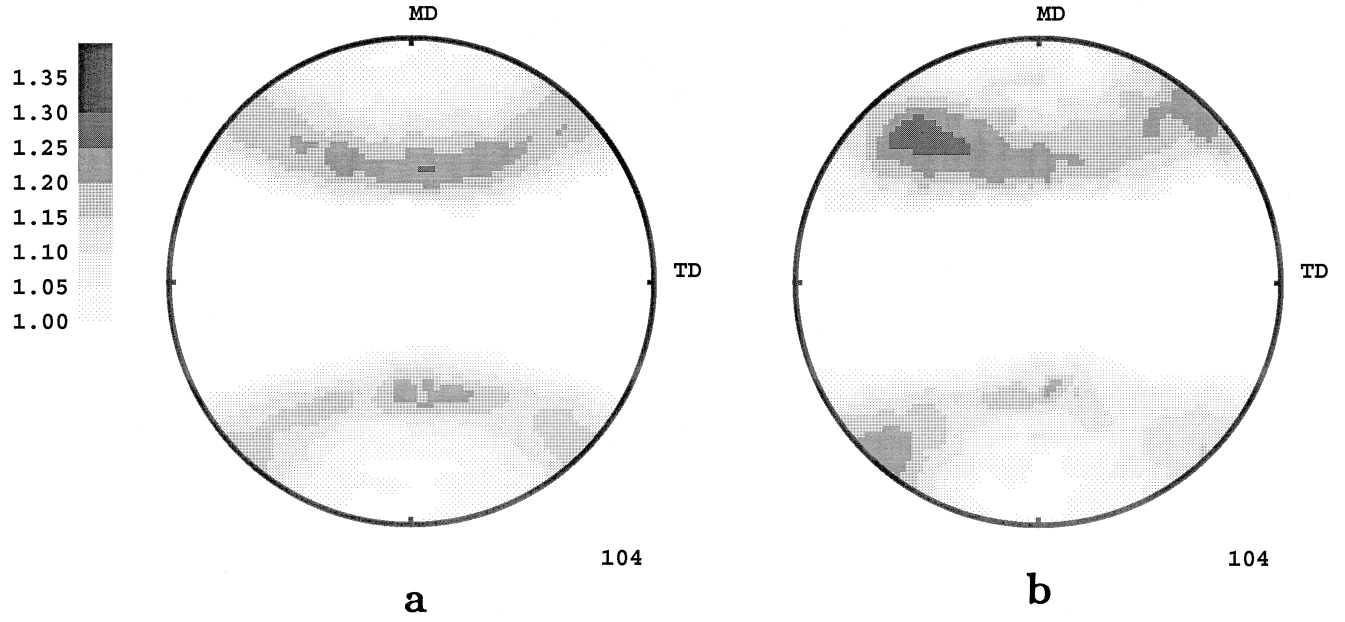

Fig. 15. Pole figures of (104) plane of calcite crystal determined for samples: (a) taken from *gate end* and (b) from *far end* of flexural bar of HDPE/CC2 75:25 blend. Flow direction is vertical. The value of 1 on the grey scale (change from white to greys) represents intensity of random specimen.

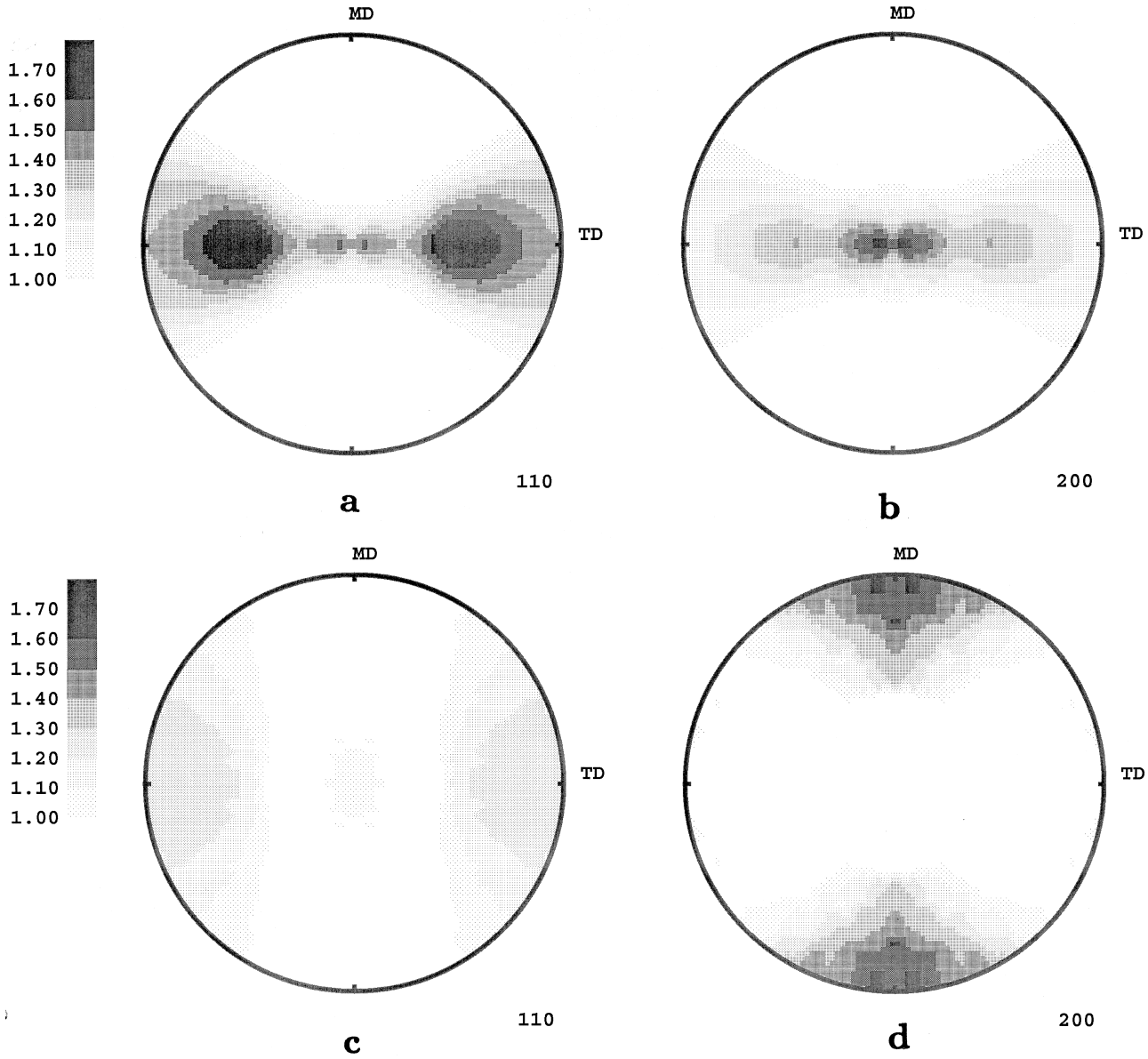

Fig. 16. Pole figures of (110) and (200) planes of polyethylene determined for samples taken from *gate end* and *far end* of flexural bar of HDPE/CC2 75:25 blend: (a) (110) plane of *gate end* sample, (b) (200) plane of *gate end* sample, (c) (110) plane of *far end* sample, (d) (200) plane of *far end* sample. Flow direction is vertical. The value of 1 on the grey scale (change from white to greys) represents intensity of random specimen.

mined for this blend from its *gate end* in Fig. 16a,b and from its *far end* in Fig. 16c,d. The orientation of polyethylene crystallites differs in both parts of the flexural bars. It is stronger and better defined in the *gate end*, but more diffuse and weaker in the *far end* specimens.

The pole figures shown in Fig. 16a,b are consistent with the orientation of the chain axis of polyethylene crystals, i.e. [001] direction along the flow direction. The intensity of the maxima is around 1.7 times the intensity of a random orientation. Thus, the orientation, while weak, is not negligible in the *gate end*. The orientation of crystallites in the *far end* specimen (Fig. 16c,d) is weaker, with the maximum intensity being only about 1.4 times that of the random intensity, is also less well developed, and suggests only a weak orientation of the molecular axis *perpendicular* to the flow direction.

The orientations of the chain axes in both halves of the flexural bars signifies the existence of a flow pattern in the mould—that was better aligned parallel to the bar axis in the *gate end* and weaker, with divergent flow (fountain effect) away from the gate. The higher orientation in the injection-moulded blends relative to that observed in neat HDPE injected under the same conditions reflects interaction of the particles with the flow field. Particles with a small aspect ratio can be expected to orient themselves along the flow direction and help create a 'flow microstructure' of better oriented polymer crystallites in the *gate end* in comparison to the neat HDPE. Evidently, such

'flow microstructure' seems to be absent in the *far end*. Clearly, this weak orientation effect resulting in the improved impact properties in the *gate end*, indicates that the 'true value' of the impact energy of an unoriented isotropic material should be somewhere between the limits given by the impact energies measured for the *gate end* and *far end* specimens. The sensitivity of the impact properties on such small orientation effects may have important practical applications in the design of injection moulds to exploit the effect to increase the toughness of industrial products.

References

[1] Knight GW. In: CB Arends, editor. Polymer toughening, ch 7. New York: Marcel Dekker, 1996:189.
[2] Pukanszky B. In: J Karger-Kocsis, editor. Polypropylene: structure, blends and composites, vol 3, Composites. London: Chapman & Hall, 1995.
[3] Baker RA, Koller LL, Kummer PE. In: HS Katz, JV Milevski, editors. Handbook of filler for plastics, 2nd ed, ch 6. New York: Van Nostrand Reinhold Co, 1987.
[4] Hoffmann H, Grellmann W, Zilvar V. In: B Sedlacek, editor. Polymer composites. New York: Walter de Gruyter, 1986:233.
[5] Badran BM, Galeski A, Kryszewski M J Appl Polym Sci 1982;27:3669.
[6] Fu Q, Wang G Polym Eng Sci 1992;32:94.
[7] Fu Q, Wang G, Shen J J Appl Polym Sci 1993;49:673.
[8] Fu Q, Wang G J Appl Polym Sci 1993;49:1985.
[9] Fu Q, Wang G Polym Int 1993;30:309.
[10] Wang Y, Lu J, Wang G J Appl Polym Sci 1997;64:1275.
[11] Bartczak Z, Argon AS, Cohen RE, Weinberg M. Polymer 1999;40:2331.
[12] Wu S J Appl Polym Sci 1988;35:549.
[13] Muratoglu OK, Argon AS, Cohen RE, Weinberg M Polymer 1995;36:921.
[14] Muratoglu OK, Argon AS, Cohen RE Polymer 1995;36:2143.
[15] Bartczak Z, Argon AS, Cohen RE, Kowalewski T. Polymer 1999;40:2367.
[16] Wunderlich B. Macromolecular physics, vol 3. New York: Academic Press, 1973.
[17] Muratoglu OK, Argon AS, Cohen RE Polymer 1995;36:4771.
[18] Chacko VP, Karasz FE, Farris RJ, Thomas EL J Appl Polym Sci 1982;20:2177.
[19] Wu X, Zhu X, Qi Z. In: The 8th International Conference on Deformation, Yield and Fracture of Polymers. London: The Plastics and Rubber Institute, 1991:78/1.
[20] Wenge Z, Qiang L, Zongneng Q J Polym Eng 1993;12:229.
[21] Argon AS. In: K Salama et al., editors. Advances in fracture research. Oxford: Pergamon Press, 1989;4:2661.
[22] Argon AS, Cohen RE, Muratoglu OK. In: MC Boyce, editor. Mechanics of plastics and plastic composites. New York: ASME. 1995:MD(vol 68)/AMD(vol 215):177.
[23] Chow TS J Polym Sci Polym Phys Ed 1978;16:959.
[24] Nicolais L, Narkis M Polymer Eng Sci 1971;11:194.
[25] Huang W-C J Composite Mater 1971;5:320.
[26] Galeski A, Argon AS, Cohen RE Macromolecules 1991;24:3953.
[27] Galeski A, Argon AS, Cohen RE Macromolecules 1991;24:3945.
[28] Lin L, Argon AS Macromolecules 1992;25:4011.
[29] Galeski A, Bartczak Z, Argon AS, Cohen RE Macromolecules 1992;25:5705.
[30] Bartczak Z, Argon AS, Cohen RE Macromolecules 1992;25:5036.
[31] Bartczak Z, Cohen RE, Argon AS Macromolecules 1992;25:4692.
[32] Bartczak Z, Argon AS, Cohen RE Polymer 1994;35:3427.
[33] Parks DM, Ahzi S J Mech Phys Solids 1990;38:701.
[34] Lee BJ, Parks DM, Ahzi S J Mech Phys Solids 1993;41:1651.
[35] Lee BJ, Argon AS, Parks DM, Ahzi S, Bartczak Z Polymer 1993;34:3555.
[36] Tzika P, Boyce MC, Parks DM, to be published.